Aperiodic Variability in the Cane–Zebiak Model: A Diagnostic Study

B. N. GOSWAMI

Centre for Atmospheric Sciences, Indian Institute of Science, Bangalore, India

J. SHUKLA

Center for Ocean–Land–Atmosphere Interactions, Department of Meteorology, University of Maryland, College Park, Maryland

(Manuscript received 12 September 1991, in final form 9 May 1992)

ABSTRACT

The finite predictability of the coupled ocean–atmosphere system is determined by its aperiodic variability. To gain insight regarding the predictability of such a system, a series of diagnostic studies has been carried out to investigate the role of convergence feedback in producing the aperiodic behavior of the standard version of the Cane–Zebiak model. In this model, an increase in sea surface temperature (SST) increases atmospheric heating by enhancing local evaporation (SST anomaly feedback) and low-level convergence (convergence feedback). The convergence feedback is a nonlinear function of the background mean convergence field. For the set of standard parameters used in the model, it is shown that the convergence feedback contributes importantly to the aperiodic behavior of the model. As the strength of the convergence feedback is increased from zero to its standard value, the model variability goes from a periodic regime to an aperiodic regime through a broadening of the frequency spectrum around the basic periodicity of about 4 years. Examination of the forcing associated with the convergence feedback reveals that it is intermittent, with relatively large amplitude only during 2 or 3 months in the early part of the calendar year. This seasonality in the efficiency of the convergence feedback is related to the strong seasonality of the mean convergence over the eastern Pacific. It is shown that if the mean convergence field is fixed at its March value, aperiodic behavior is produced even in the absence of annual cycles in the other mean fields. On the other hand, if the mean convergence field is fixed at its September value, the coupled model evolution remains close to periodic, even in the presence of the annual cycle in the other fields.

The role of convergence feedback on the aperiodic variability of the model for other parameter regimes is also examined. It is shown that a range exists in the strength of the SST anomaly feedback for which the model variability is aperiodic even without the convergence feedback. It appears that in the absence of convergence feedback, enhancement of the strength of the air–sea coupling in the model through other physical processes also results in aperiodicity in the model.

1. Introduction

In recent years, many observational aspects of the interannual variation associated with the El Niño/Southern Oscillation (ENSO), especially those in the tropical Pacific, have been documented rather extensively (Rasmusson and Carpenter 1982; Cane 1986; Rasmusson and Wallace 1983; Rasmusson and Arkin 1985; Wright et al. 1988). One of the important characteristics of the ENSO phenomenon is the irregular recurrence of warm events in the central and eastern Pacific with a preferred periodicity of 3–4 years. The role of coupling between the ocean and the atmosphere to explain this interannual variability was already recognized by Bjerknes (1969). However, early attempts to simulate the ENSO-type interannual variability using coupled ocean–atmosphere models (McCreary 1983; McCreary and Anderson 1984; Anderson and McCreary 1985) did not reproduce the *aperiodic* nature of the phenomenon. Recently, Cane and Zebiak (Cane and Zebiak 1985, 1987; Cane et al. 1986; Zebiak and Cane 1987) developed a simple coupled model (hereafter referred to as a CZ model) that is successful in simulating both the preferred periodicity of 3–4 years and the irregular intervals between events. The CZ model is an anomaly model, yet it apparently contains the basic physics of the problem. The ocean evolves according to linear reduced-gravity equations and has a frictionally driven, constant-depth, upper mixed layer. The atmospheric model dynamics is that of Gill (1980). The seasonal cycle is included through prescribed climatological surface winds, sea surface temperature (SST), and ocean currents. The SST anomalies (SSTA) are predicted by a fully nonlinear thermodynamic equation. The atmosphere is coupled to the ocean through the surface wind stress and param-

Corresponding author address: Dr. B. N. Goswami, Centre for Atmospheric Sciences, Indian Institute of Science, Bangalore, 560 012 India.

eterized by a drag law and through atmospheric heating, whose parameterization has two parts. One part is proportional to the SSTA (SSTA feedback) but depends nonlinearly on the mean SST. The other part is proportional to the convergence anomaly (convergence feedback) but operates only when the total flow is convergent. In this manner, the coupling depends on the annual cycles of the mean convergence and SST. The model has several attributes and adjustable parameters, such as oceanic equivalent depth, the sharpness and amplitude of the mean thermocline, the strength of atmospheric heating proportional to the SSTA, the strength of the atmospheric heating proportional to the low-level convergence anomaly, and atmospheric friction. Zebiak and Cane (1987, 1988) have shown that the model's variability does depend on these parameters to some extent. However, for a range of parameters the model simulates several features of the observed ENSO variability reasonably well. We shall call the set of parameters used in Zebiak and Cane (1987) the *standard* set. According to Cane and Zebiak (Cane et al. 1987; Cane and Zebiak 1987; Zebiak and Cane 1987), the ENSO cycles depend on variations of the zonal-mean heat content of the equatorial ocean. The interval between events is related to the refill time of the equatorial heat reservoir. According to them, free equatorial waves alone do not determine this refill time.

Following a somewhat different route, Schopf and Suarez (1988) developed a fully nonlinear coupled ocean–atmosphere model. Their atmospheric model is a two-level primitive equation model on a sphere described by Held and Suarez (1978). No water vapor is included, and the model is driven by relaxing the mean atmospheric temperature toward a zonally symmetric state with a large pole-to-equator temperature difference. The ocean is also a two-layer primitive equation model, including thermodynamic budgets developed by Schopf and Cane (1983) and modified by Schopf and Harrison (1983). The coupling is through a linear relationship between SST and heating. In a 35-year integration of the coupled model, Schopf and Suarez (1988) found low-frequency ENSO-like variability with time scales of 3 to 5 years. The occurrence of warm events is rather aperiodic and there is no asymmetry between warm and cold events in their model. Through experimentation with the model, they have established that the irregularity in their model simulations occurs mainly from the "noise" generated by nonlinearities in the atmospheric component of the model. When they couple a linear version of the atmospheric model to the nonlinear ocean model, the coupled model's variability is strictly periodic. This version of the Schopf and Suarez model is similar to the CZ model in that a linear atmosphere model is coupled to a nonlinear ocean model. However, the atmospheric heating in their model is proportional to the SSTA alone and the part proportional to the low-level convergence anomaly is absent.

Battisti (1988) also developed a coupled model very similar to the one developed by Zebiak and Cane (1987). Surprisingly, however, he could get only regular periodic oscillations in the model simulations. Detailed investigation of the model results by Battisti (1988) and Battisti and Hirst (1989) has identified the physical mechanism responsible for the periodicity or the growth and decay of the warm events in Battisti's model. They show that the initial downwelling warming signal during an El Niño year grows slowly in place (due to coupled instability) in the eastern Pacific. At the same time, an upwelling signal is excited in the central Pacific that propagates to the western boundary in the form of the gravest meridional Rossby wave, returns to the warming area as an equatorially trapped Kelvin wave, and destroys the downwelling signal, thus ending the warm ENSO phase. The periodicity of the phenomenon is determined by a combination of the growth rate of the instability (determined by various thermodynamic processes in the region) and the travel time of the Rossby–Kelvin wave back to the warming region (determined by the equatorial ocean hydrodynamics and the size of the basin). Based on these studies, Battisti and Hirst (1989) have proposed a delayed oscillator model for the evolution and decay of ENSO events. Independently, Suarez and Schopf (1988) have also proposed a similar delayed oscillator mechanism for ENSO variability.

While these studies have advanced our understanding of the dynamics and thermodynamics of warm events and have proposed a quite plausible scenario in which periodic warming and cooling can take place, the origin of the aperiodic nature of these events as in the CZ model is not fully explained. Recently, we examined the predictability of the CZ model (Goswami and Shukla 1991). It was shown that the growth of small errors in the model is governed by two time scales: one fast time scale with an *e*-folding time of about 6.5 months and another slow time scale with an *e*-folding time of about 21 months. The limit on the predictability of the CZ model is a manifestation of the aperiodic variability of the model. Therefore, it is important to understand the origin of the latter. We have carried out a series of diagnostic experiments to address this problem. A comparison between variability in Battisti's model (Battisti 1988) and that in the CZ model (Zebiak and Cane 1988) shows that they simulate the same low-frequency variability but the frequency spectrum in the latter model is somewhat broader around the dominant periodicity. Battisti (1989) showed that aperiodic variability similar to that in the CZ model may be obtained in his model if a small amount of high-frequency noise is introduced. Our primary objective is to identify the source of such a high-frequency component in the standard version of the CZ model. A high-frequency response can arise from the nonlinearities in the model. The model has explicit advective nonlinearities in the thermodynamic

equation and has implicit nonlinearities associated with the coupling processes. In section 2, sensitivity studies are carried out to isolate the source of the high-frequency component in the standard case. In section 3, the nature of the forcing associated with the convergence feedback is investigated. It is also shown in this section that the convergence feedback is just one way of producing this high-frequency component. In the absence of the convergence feedback, an increase in the air–sea coupling strength through the enhancement of the SSTA feedback is another way to make the model variability aperiodic. The results are summarized in section 4. Section 5 presents our conclusions and a discussion of how we arrived at them.

2. Model sensitivity

In Goswami and Shukla (1991), a *control* run was discussed that was obtained by forcing the ocean model with the observed surface wind stresses. The wind-stress anomalies used in this control run are based on subjective analyses of monthly mean surface wind obtained from ship reports (Goldenberg and O'Brien 1981). The analyzed winds were filtered and detrended as discussed by Cane et al. (1986). The ocean model was forced by these observed wind-stress anomalies from January 1964 to May 1988. Starting from January 1970, the coupled model fields were saved every month. The initial conditions for our sensitivity experiments are taken from this *control* run. These initial conditions corresponding to any month t_o consist of ocean currents, thermocline depth, and SST anomalies that were forced by the observed surface winds from January 1964 to t_o. The atmospheric winds and geopotential perturbations at t_o are the result of the atmospheric response to the SST anomalies at that instant. By saving these initial conditions, we avoid repeated integration of the ocean model in the forced mode from January 1964 every time we want an initial condition.

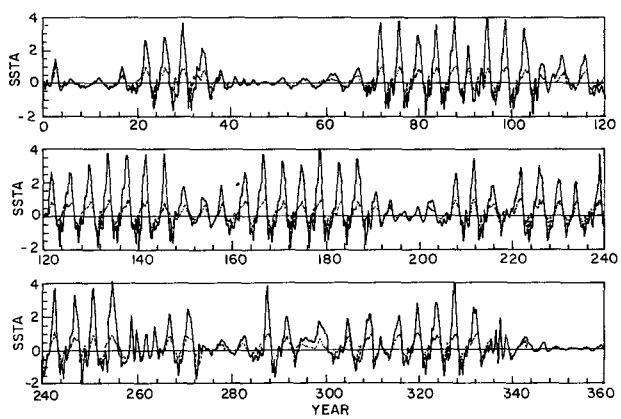

FIG. 1. Time series of area-averaged SSTA from the standard run for 360 years with convergence feedback (α = 1.6, β = 0.75, and I_{max} = 2). The solid curve is for NINO3 (5°N–5°S, 90°–150°W) and the dashed curve is for NINO4 (5°N–5°S, 150°W–160°E).

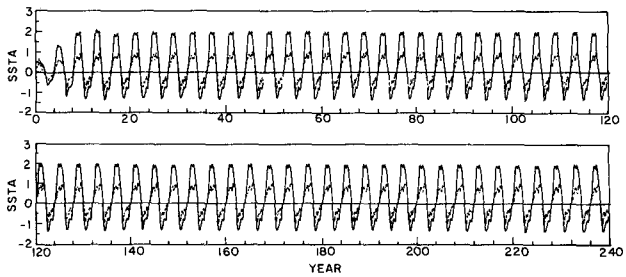

FIG. 2. Time series for the same area-averaged SSTA as in Fig. 1, for a 240-year integration without the convergence feedback (β = 0). All other parameters are the same as in Fig. 1.

In the CZ model, atmospheric heating is represented by two terms. These two terms are parameterized as

$$\dot{Q}_s = (\alpha T)\exp[(\bar{T} - 30°\text{C})/16.7°\text{C}] \quad (1)$$

and

$$\dot{Q}_1^n = \beta[M(\bar{c} + c^n) - M(\bar{c})], \quad (2)$$

where

$$M(x) = \begin{cases} 0 & x \leq 0 \\ x & x > 0. \end{cases} \quad (3)$$

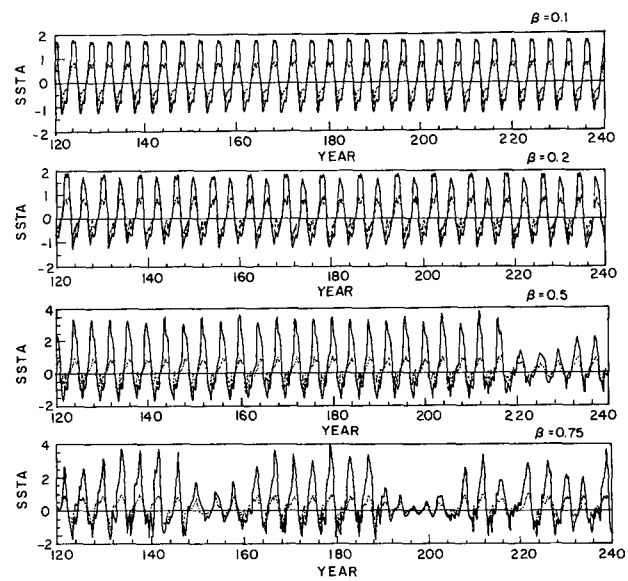

FIG. 3. Time series of the same area-averaged SSTA as in Fig. 1, but from four experiments with increasing strength of the convergence feedback. Each experiment was integrated for 240 years, and the evolution for the last 120 years is shown in each case; α = 1.6 in each of these cases.

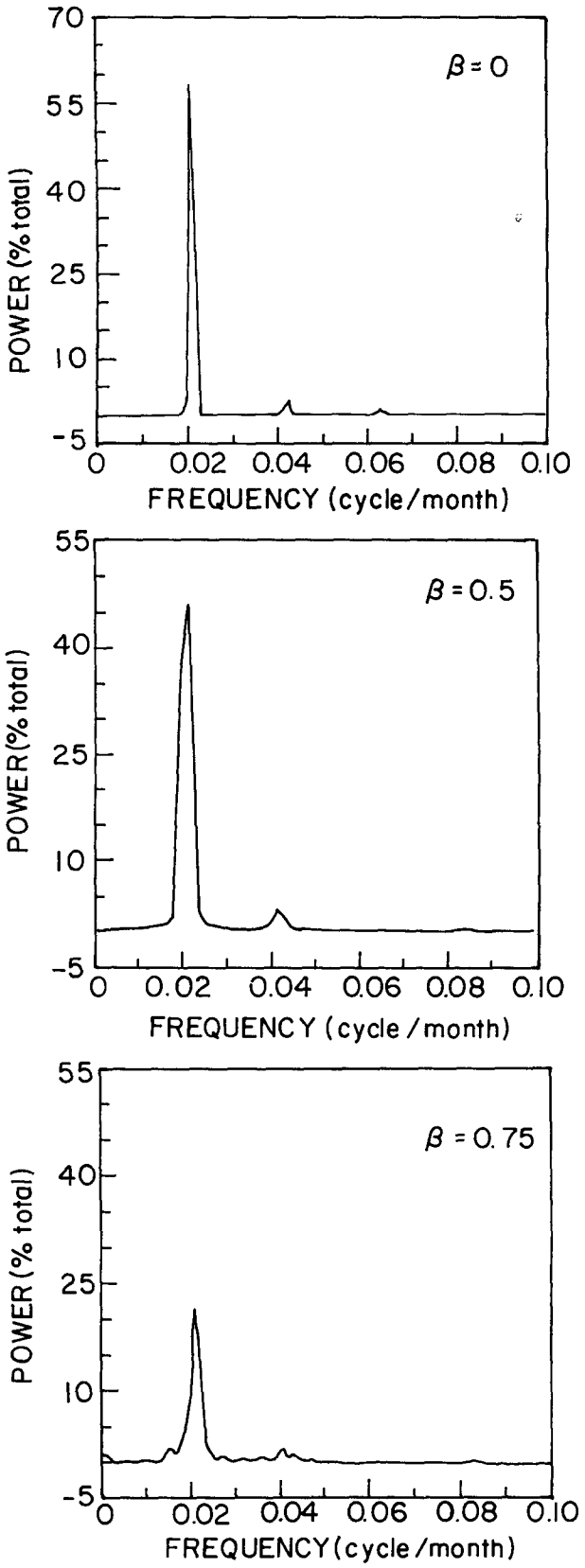

FIG. 4. Power spectrum of NINO3 SSTA from three simulations with three different values of the strength of the convergence feedback (β). Power is shown as percentage of the total power and unit for frequency is cycles per month.

The first term ($\dot{Q}_s$) represents the component of atmospheric heating associated with the increase in local evaporation due to the increase in SST (T) and is a function of the prescribed climatological monthly mean SST ($\bar{T}$). The feedback represented by this part is termed as the SST anomaly (SSTA) feedback. The second term ($\dot{Q}_1^n$) represents the component of atmospheric heating due to increased low-level convergence associated with the SSTA-induced heating. The feedback associated with this part of the heating is termed as the convergence feedback. The term $\bar{c}$ in Eq. (2) is the prescribed climatological monthly mean convergence, and c^n is the anomaly convergence induced by the SST anomalies in the n^{th} iteration. In the CZ model, this part is calculated iteratively with a limit $I_{\max}$ on the maximum number of iterations. The terms α and β represent the strength of the coupling processes corresponding to SSTA feedback and convergence feedback, respectively. In the standard version of the CZ model, the dimensional values of α and β are 0.031 $m^2\ s^{-3}/°C$ and $1.6 \times 10^4\ m^2\ s^{-2}$, respectively, and $I_{\max}$ is 2. The corresponding nondimensional values of α and β are 1.6 and 0.75, respectively. As the anomaly convergence is essentially produced by the SST anomalies, the location of c^n is closely related to the location of the SST anomalies. If this location happens to be a location of climatological-mean divergence, however, it does not produce any heating. In this manner, the feedback is nonlinearly dependent on the climatological-mean convergence. The value of $I_{\max}$ is set by CZ based on their experimentation with this limit. It is found that an increase in the number of iterations does not result in any qualitative change in the model variability. In this section, results are first presented from a *standard* run and then the sensitivity of the model's variability to changes in the two coupling processes is examined.

a. The standard case: Both SSTA and convergence feedback

To have a frame of reference for the model's natural variability, we carried out a long integration (480 years) of the coupled model with standard values of the parameters ($\alpha = 1.6$, $\beta = 0.75$, and $I_{\max} = 2$). The basic states used in the standard case are the same as those in Zebiak and Cane (1987). The observed climatological surface winds and SST are used. Mean ocean currents are generated by spinning up the ocean model with monthly mean climatological winds. The time evolution of the area-averaged SSTA over NINO3

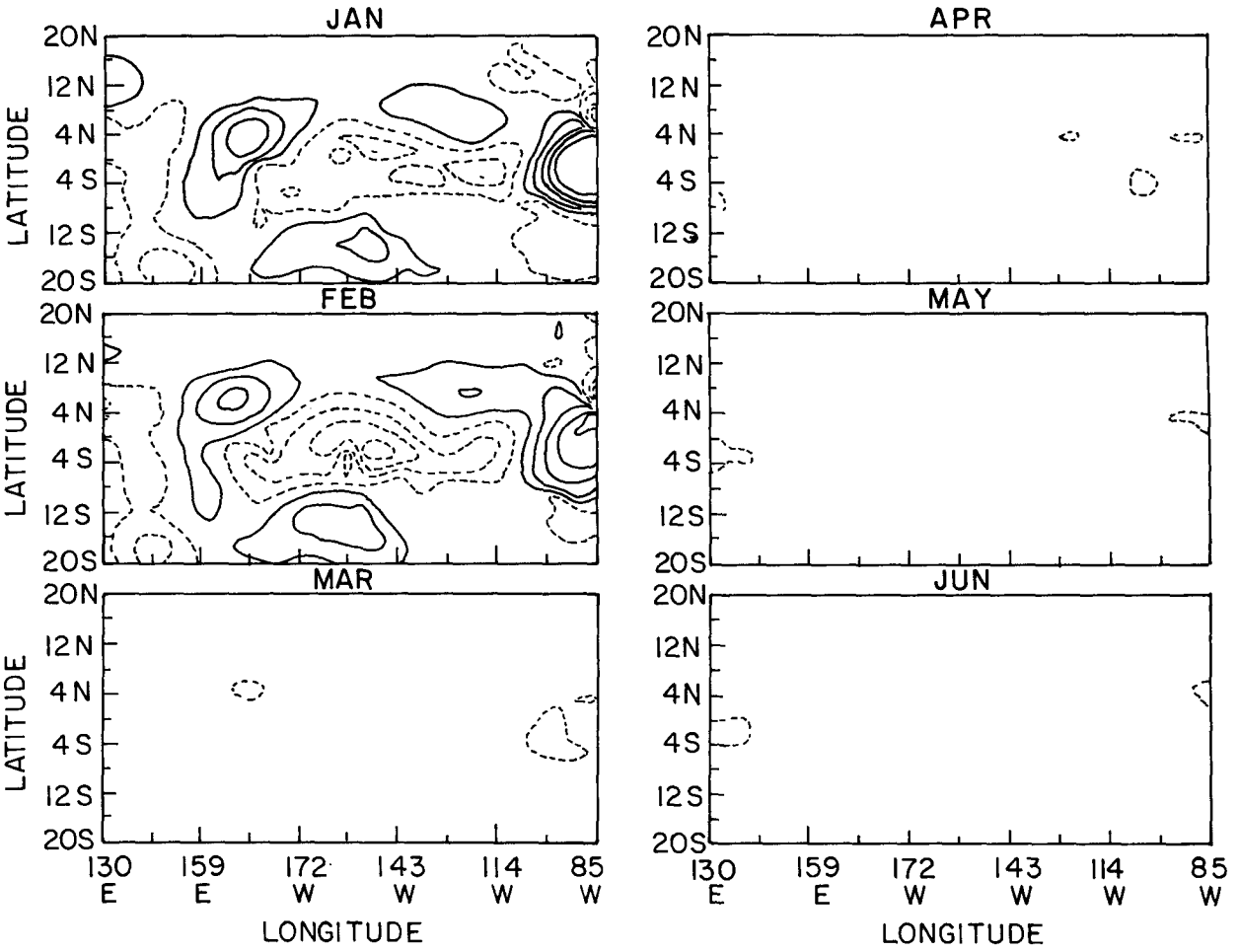

FIG. 5. Difference (with convergence feedback–without convergence feedback) in divergence anomalies between two 10-day coupled model simulations, one with and the other without the convergence feedback. The 12 panels correspond to initial conditions from the 12 months of 1981. Contour interval is 0.15 and the unit is in 1×10^{-6} s^{-1}. The negative contours are dashed lines. The first negative contour is −0.05 and the first positive contour is 0.1. The zero contour is not plotted.

(5°N–5°S, 90°W–150°W) and NINO4 (5°N–5°S, 160°E–150°W) for the first 360 years is shown in Fig. 1. Highly aperiodic behavior of the evolution is evident, apart from certain other striking features. First, there are often long periods of inactivity, such as between years 4 and 20 and between years 40 and 60. Second, there is a favored periodicity of about 4 years, with an asymmetry between the amplitudes of mature warm and cold events. Other details of the variability of the model's evolution are discussed at length by Zebiak and Cane (1987, 1988).

b. No convergence feedback and standard SSTA feedback

Next, we conducted a coupled model experiment with the standard strength of the SSTA feedback ($\alpha = 1.6$) but with the convergence feedback eliminated by setting $\beta = 0$. The evolution of the same area-averaged quantities are shown in Fig. 2 for 240 years. It is clear that the absence of the convergence feedback makes the model periodic after a short initial period of adjustment. The periodicity is nearly 4 years. Integrations with a number of other initial conditions show that without the convergence feedback the model always settles down to a similar periodic state. The initial adjustment period ranges from 5 to 10 years for different initial conditions. Thus, it is clear that the fundamental periodicity of about 4 years is a result of equatorial ocean dynamics and SSTA feedback to the atmosphere. The aperiodic behavior of the model in the standard case results mainly from the nonlinearities associated with the convergence feedback.

To understand the transition from periodic to aperiodic behavior in the model, we carried out a series of integrations by gradually increasing the strength of the convergence feedback (i.e., by increasing the value of β). The area-averaged SSTA over NINO3 and

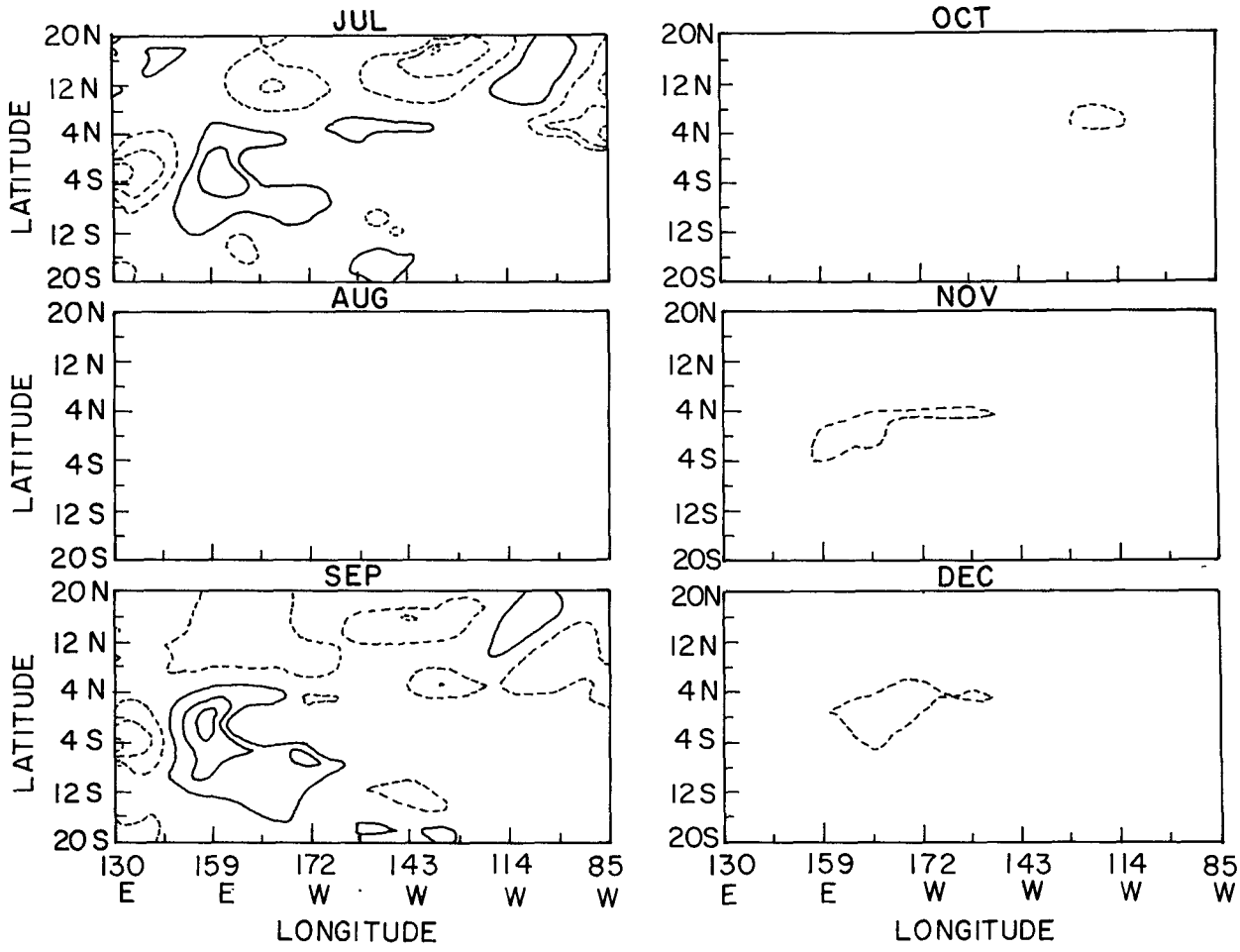

FIG. 5. (*Continued*)

NINO4 for four such experiments with β corresponding to 0.1, 0.2, 0.5, and 0.75, respectively, is shown in Fig. 3. The time evolution of the last 120 years of each 240-year integration is shown. It is seen that, for weak convergence feedback ($\beta = 0.1$ or 0.2), the model evolution remains close to the periodic mode. For moderate strength of the convergence feedback (e.g., $\beta = 0.5$), the model evolution becomes quasi-periodic with more than one—but a finite number of—frequencies present. For stronger convergence feedback (e.g., $\beta = 0.75$ as in Fig. 1 and in the last panel of Fig. 3), the model evolution becomes aperiodic with many frequencies present.

The evolution of the model with convergence feedback as strong as or stronger than the standard case is clearly aperiodic. To describe the transition to aperiodic behavior more quantitatively, we examined the power spectrum of the NINO3 SSTA time series corresponding to a number of values of β. The spectra of NINO3 SSTA, for β corresponding to 0.0, 0.5, and 0.75, are shown in Fig. 4. As expected, in the absence of the convergence feedback ($\beta = 0$), there is only one dominant frequency with period between 48 and 49 months. Two minor periodicities with periods of 24 and 16 months are also seen. It is interesting to note that the fundamental frequency with a period of about 48 months remains the dominant frequency even at high values of β. However, as the strength of the convergence feedback is increased, a line broadening takes place around the fundamental frequency. For example, in the standard case ($\beta = 0.75$), almost all periods between 40 months and 75 months are found to have significant amplitude.

3. Insight regarding the convergence feedback

It appears from Figs. 3 and 4 that the convergence feedback introduces a high-frequency component to the basic approximate 4-year periodicity of the system. The broadening of the spectrum arises due to the nonlinear interaction between these two low- and high-frequency components. To understand how the convergence feedback forcing operates, the difference between two runs was examined, one with convergence

feedback and the other without it, during very early phases of their evolution. Two sets of 10-day integrations (one time step in the CZ model) were carried out, one with convergence feedback and one without, for all 181 initial conditions corresponding to January 1970 through January 1985. Then the differences (with feedback minus without feedback) in different fields between the two runs were calculated. The differences in the anomaly divergence field are illustrative. As an example, the differences in the divergence anomaly for initial conditions corresponding to January 1981 through December 1981 are shown in Fig. 5. The negative contours represent areas where there was more convergence in the convergence feedback case compared to the case without convergence feedback. It is seen that during eight months of the year there were hardly any differences between the two cases. Major differences in the divergence anomaly over the central and eastern equatorial region occur during January and February. Some differences over the western equatorial region are seen during August and October. This picture is representative of other years, where major differences in central and eastern equatorial divergence anomalies occur in northern winter and early spring (December–April) and some differences in western equatorial divergence anomalies occur in northern autumn. This seasonal dependence of the convergence feedback forcing is further illustrated in Fig. 6, where the differences in divergence anomalies averaged between 5°N to 5°S are shown for all longitudes and for all initial conditions. We note that in most of the years, the convergence feedback is effective only during the early part of the calendar year. The difference of the anomaly convergence field also shows the existence of a certain amount of high-frequency variability.

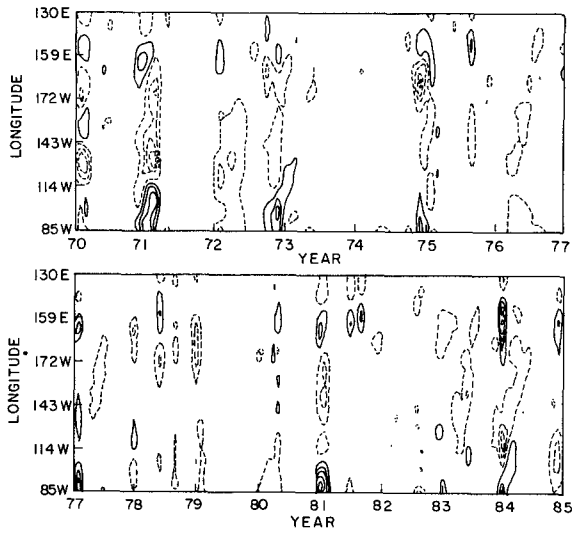

FIG. 6. Time–longitude section of the divergence anomaly difference between two 10-day coupled model simulations, one with and the other without the convergence feedback, averaged over 5°N to 5°S latitude belt. The unit, contour interval, and contouring convention are the same as in Fig. 5.

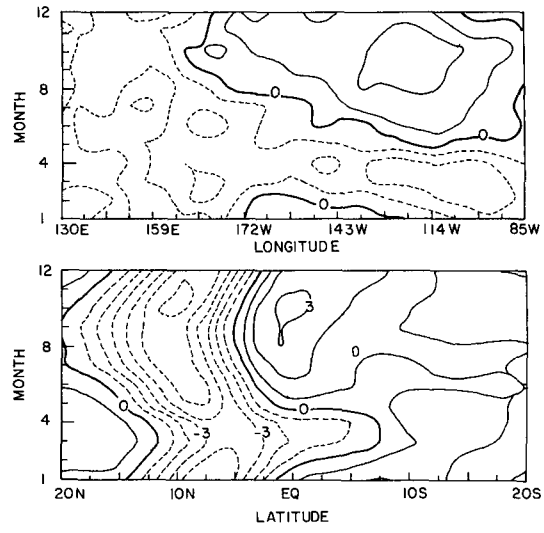

FIG. 7. The seasonal cycle of the climatological-mean convergence. The upper panel contains time [Jan (month 1) to Dec. (month 12)]–longitude section averaged between 5°N and 5°S. The lower panel contains time–latitude section averaged over the eastern Pacific (160°W and 90°W). The negative contours are dashed and the contour interval is 1×10^{-6} s^{-1}.

Thus, the heating associated with the convergence feedback has a tendency to be effective only during a certain phase of the annual cycle. From Eq. (2), we note that the largest response to the convergence feedback takes place if positive SSTA occurs in the region of mean convergence. The largest positive SSTA occurs over the central and eastern equatorial Pacific. It is also clear from Fig. 7 that the mean convergence field has a clear annual cycle in the eastern part of the Pacific. In particular, the mean field is convergent in this region only during the early part of the calendar year. We believe this is primarily why the heating associated with the convergence feedback tends to be locked to a particular phase of the annual cycle. In the following, we describe results of a series of controlled experiments designed to provide further insight into the working of the convergence feedback.

a. Perpetual March and September mean convergences; all other mean fields have normal annual cycle

As discussed earlier in this section, the convergence feedback is intimately related to a particular phase of the annual cycle of the mean convergence field. The question then arises as to how crucial the role of the annual cycle is in producing the high-frequency component. Is the annual cycle in the mean convergence field necessary in generating the high-frequency component? What role does the annual cycle of the other

mean fields play in generating the high-frequency component? Is the annual cycle in the absence of the convergence feedback sufficient to generate it? The following controlled experiments are carried out to provide some answers to these questions. For example, February–March–April are the months (Fig. 7) when the mean convergence field is located south of the equator and thus has the greatest chance to enhance the heating through convergence feedback. On the other hand, in August–September–October the convergence field is farthest to the north and has the least chance of contributing to the heating field via convergence feedback. Thus, if our hypothesis is right, a perpetual March mean convergence field should be more conducive to introducing a high-frequency component than a perpetual September mean convergence field.

In the next experiment, the mean convergence field was held fixed at its March values while all other mean fields have their normal annual cycle. The model was integrated for three different strengths of the convergence feedback (β = 0.2, 0.5, 0.75). The results are shown in Fig. 8. It is remarkable to note that in this case even for weak convergence feedback (β = 0.2), the variability is chaotic. This experiment was repeated with the mean convergence field held fixed at September values. These results are shown in Fig. 9. In this case, it is clearly seen that the variability remains quasi-periodic even for large strength of the convergence feedback (β = 0.75). It is clear from these two experiments that the convergence feedback is unable to produce the high-frequency component if the mean convergence is held fixed at September values, while it can produce a high-frequency component even at a small strength of coupling if the mean convergence field is held fixed at March values. The experiments also show that the high-frequency part basically comes from the coupling and the annual cycle in the mean convergence only provides the right environment some time during the year for generating this high-frequency component.

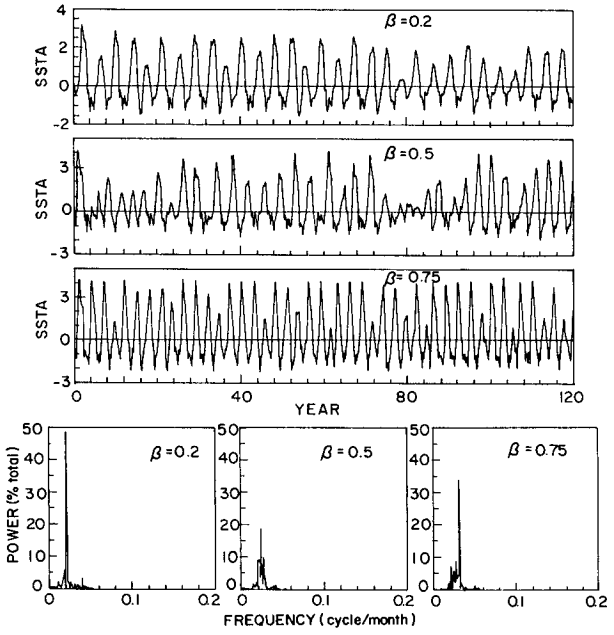

FIG. 8. Time evolution of NINO3 SSTA (°C) corresponding to three different strengths of the convergence feedback (top three panels) when the mean convergence field is kept fixed at March values. The other mean fields have the normal annual cycle. The power spectrum corresponding to the three different time series are shown below.

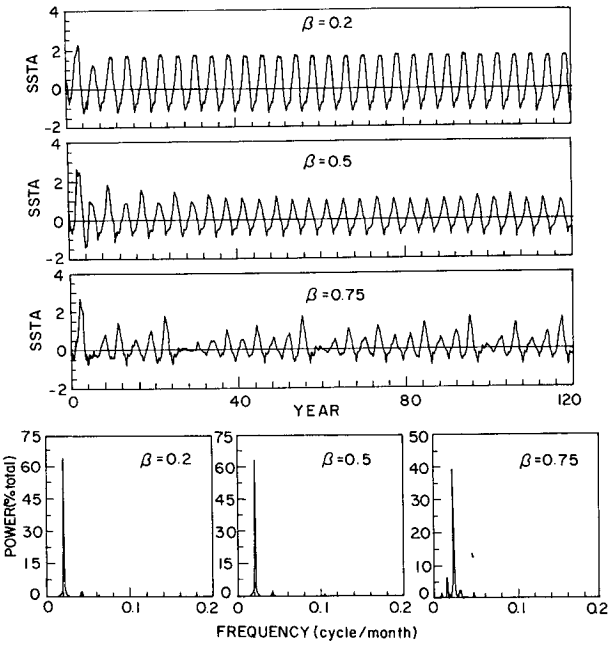

FIG. 9. Same as Fig. 8 except when the mean convergence field is held fixed at September values.

The wind-stress anomaly is dependent on the annual cycle of the mean surface winds. Since the wind stress is a nonlinear function of the winds, it can be argued that the annual cycle in the mean surface wind interacting through the surface wind stress may generate high-frequency noise in the model. To test this we carried out one experiment in which the mean surface winds are fixed at March values. The mean divergence is also fixed at March value, while all other fields vary annually. The results of this experiment are shown in Fig. 10. It is interesting to note that this figure is quite similar to Fig. 8. Comparing the power spectra of the time series in Fig. 8 and Fig. 10, we note that the spectrum contains more high-frequency signals in Fig. 10 as compared to those in Fig. 8. This indicates that the removal of the annual cycle of the mean surface winds, in fact, helps the convergence feedback to enhance the aperiodicity of the model. It further supports the idea that the aperiodicity in the standard version of the CZ model is introduced primarily by the convergence feedback.

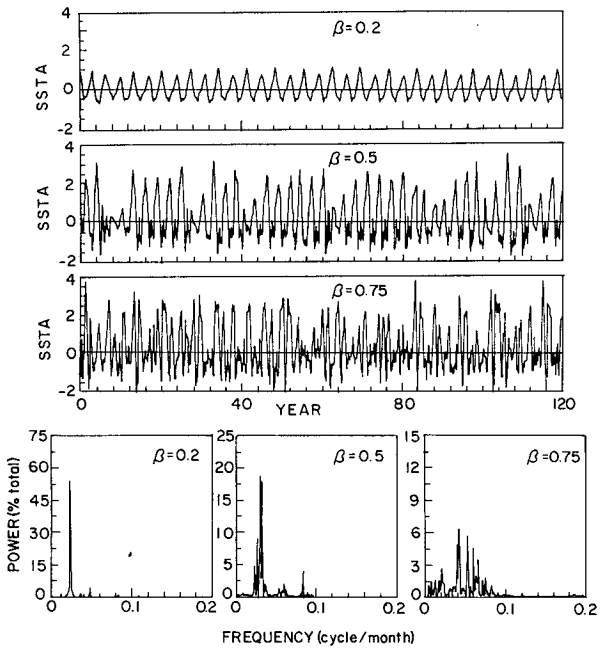

FIG. 10. Same as Fig. 8 except that both the mean convergence and mean surface winds are kept fixed at March values in this experiment. The rest of the mean fields have their normal annual cycle.

b. *Role of the annual cycles in the atmospheric mean fields other than the convergence field*

To examine the role played by the annual cycle in the mean fields other than the convergence field in producing the aperiodicity of the model, we carried out one set of integrations in which the mean convergence field had its normal annual cycle while all other mean fields were fixed at their annual mean value. The results are shown in Fig. 11. In this case, the model behavior is chaotic even for $\beta = 0.5$. The nature of the variability is very similar to that of the standard case (Fig. 3) in which all the mean fields had their annual cycle. In fact, in the presence of the annual cycle of all the mean fields, the variability for moderate strength of the convergence feedback ($\beta = 0.5$) is quasi-periodic (Fig. 4), while in the absence of the annual cycle of the mean fields other than the mean convergence field, the variability for the same strength of the convergence feedback is quite chaotic. In other words, the annual cycle of the mean fields other than the mean convergence helps to suppress only a part of the high-frequency component generated by the convergence feedback.

c. *Enhanced SSTA feedback without convergence feedback*

We discussed earlier that the convergence feedback represents the strength of a component of the air–sea coupling. As we have demonstrated, the coupled model's behavior depends sensitively on the convergence feedback. It may be logical to ask whether the model behavior depends sensitively on all parameters that determine the strength of the air–sea coupling. Apart from the convergence feedback, another parameter that influences the strength of the air–sea coupling is α, the strength of the SSTA feedback [see Eq. (1)]. Therefore, in this section, we examine whether the model behaves aperiodically even in the absence of convergence feedback but for enhanced air–sea coupling through increased strengths of the SSTA feedback (α). We carried out four experiments with $\beta = 0$ and with $\alpha = 1.7$, 1.8, 1.9, and 2.0, respectively. The results of these experiments are shown in Fig. 12. It is interesting to note that for $\alpha \geqslant 1.8$, the interannual variability is chaotic. However, if α is increased further (not shown) for $\alpha \gtrsim 2.2$ the interannual variability again becomes periodic. It is found that for larger α, the amplitude of the interannual oscillations is larger. Moreover, the period of the interannual oscillations for large α is longer. It is seen that for $\alpha = 2.0$, the dominant periodicity has already shifted to about 60 months. Zebiak and Cane (1987) also found that a small increase in the air–sea coupling strength (α) increases the amplitude of the interannual oscillations. Battisti and Hirst (1989) show that the interannual variability of the coupled model may be described by a simple delayed-oscillator analog model. They also show that an increase in the local instability increases the period of the system if the other parameters remain constant. An increase in the strength of the air–sea coupling α is responsible for an increase in the local instability (Hirst 1986). The results of our sensitivity studies are consistent with the results of these conceptual models.

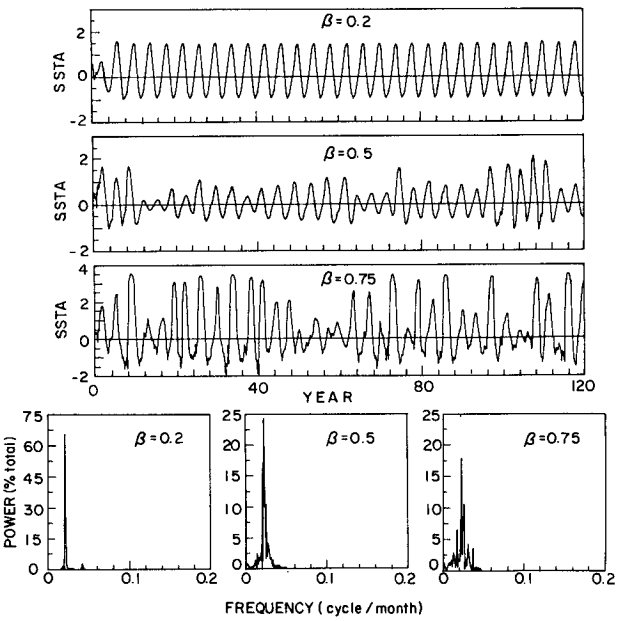

FIG. 11. Same as Fig. 10 but the mean convergence field has its annual cycle while all other mean fields are fixed at their annual mean values.

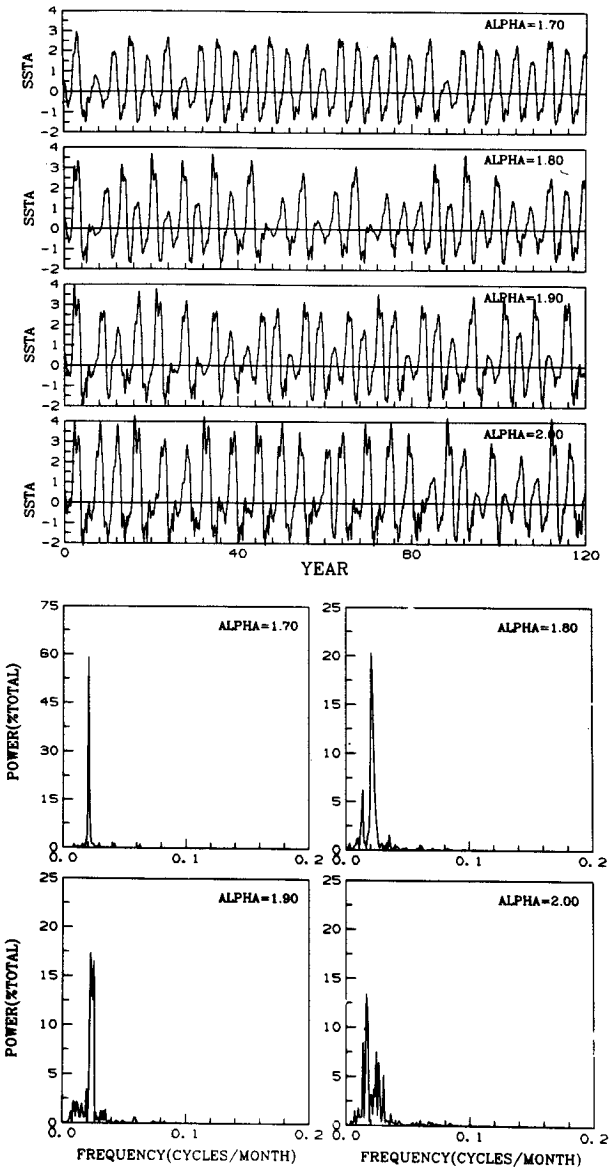

FIG. 12. The evolution of NINO3 SSTA (°C) in four experiments in which there was no convergence feedback ($\beta = 0$) but the strength of the SSTA feedback was increased from $\alpha = 1.6$ to $\alpha = 1.7$, 1.8, 1.9, and 2.0, respectively. All mean fields have their normal annual cycle. The power spectrum corresponding to each series is shown below.

Figure 12 shows that even in the absence of convergence feedback the model variability could be aperiodic if the air–sea coupling is increased suitably through an increase in the strength of SSTA feedback. While the increase in the amplitude and period may be understood in the framework of an analog model, the origin of the aperiodicity in this case is not obvious.

4. Conclusions and discussion

We have investigated the origin of the aperiodic behavior in the coupled model developed by Zebiak and Cane (1987) and have shown that in the standard case the forcing associated with the convergence feedback is responsible for this behavior. In the absence of convergence feedback, the model variability is highly periodic, with a period of nearly 4 years. As the strength of the convergence feedback is increased, the model's variability goes from a periodic to an aperiodic regime. This happens through a gradual broadening of the spectrum of the model's variability around the basic frequency. Thus, even in the standard case, where the variability is clearly aperiodic (Fig. 1), the 4-year periodicity is still dominant. However, the convergence feedback introduces a high-frequency component in the model's variability. It is the nonlinear interaction between the high frequencies and the basic low frequency that makes the evolution aperiodic. A detailed investigation of the nature of the forcing associated with convergence feedback shows that it is effective only for 2–3 months, mostly during the early part of the calendar year. This is because the convergence feedback is effective only if the background wind field is convergent in the region of positive SST anomalies. The south equatorial Pacific is the region where the ocean dynamics creates significant positive SST anomalies. Therefore, the convergence feedback can enhance the atmospheric heating only during early spring, as this is the period when the mean convergence zone crosses to the south of the equator in the eastern Pacific.

We also investigated whether the annual cycle in the mean convergence is essential for the generation of the high-frequency component in the standard model. We showed that an "annual cycle" in the mean convergence field is not essential for the aperiodic behavior of the model. In fact, if the mean convergence field is fixed at March values, the model behavior becomes aperiodic even for a small strength of the coupling. On the other hand, if the mean convergence is fixed at September values or at annual mean value, the model behavior remains periodic until the strength of coupling is high. The annual cycle essentially produces favorable conditions for 2–3 months each year for the convergence feedback to generate the high-frequency component.

Our results are supported by recent findings of theoretical studies by Goswami and Selvarajan (1991), who carried out a linear stability analysis of the coupled system similar to the one used by Hirst (1986, Model III) in which the convergence feedback was also included in the parameterization of the atmospheric heating. It was found that the convergence feedback enhances the growth of the low-frequency unstable mode found by Hirst, and also introduces a set of new unstable higher-frequency intraseasonal modes whose growth rates are nearly independent of the wavenumber. For reasonable values of the parameters, the growth rates of the new higher-frequency unstable modes are smaller than those of the low-frequency mode. Thus, we can speculate that the aperiodicity in the CZ model is a result of nonlinear interaction between the low-

frequency dominant mode with the "white noise" weakly unstable high-frequency modes introduced by the convergence feedback. Battisti and Hirst (1989) showed that the low-frequency periodic part of the CZ model variability may be represented by a nonlinear delayed-action oscillator analog model. They also showed that a small amount of high-frequency external forcing with white noise spectrum broadens the basic low-frequency spectra and makes the variability aperiodic. In the present study we have essentially identified the source of the high-frequency noise in the standard CZ model.

It is known that the predictability of the CZ model has a seasonal dependence (Cane et al. 1986; Goswami and Shukla 1991). In particular, Goswami and Shukla (1991) show that growth of errors is fastest between March and May and slowest between September and January. It is seen from Fig. 7 that March–May is the time when the mean convergence occurs over the equatorial eastern Pacific. Hence, this is the time when the convergence feedback could introduce "noise" in the coupled system and degrade predictability. Thus, our analysis illustrates the cause for seasonality of predictability of the CZ model.

The parameterization of the convergence feedback assumes that SST anomalies increase the low-level convergence by generating deep heat sources in the atmosphere. This may be possible when the mean background SST is high ($\geq 28°C$). However, most of the positive SST anomalies in the model occur in the eastern half of Pacific, where the mean SST is lower. In fact, Lindzen and Nigam (1987) suggest that the gradient of the SST rather than the SST anomalies may be important in producing the low-level convergence in such a case. Therefore, we also examined whether convergence feedback is essential for the model to have aperiodic variability in other parameter regimes and showed that it is not essential. In the absence of the convergence feedback ($\beta = 0$), one way in which the model can have aperiodic variability is by increasing the air–sea coupling associated with the SSTA feedback (α). It is shown that as the strength of this coupling is increased, the model goes from a periodic to a chaotic regime. A further increase in the strength of the coupling, however, takes the model back to another periodic regime.

Acknowledgments. The authors thank Drs. Mark Cane and Steve Zebiak for kindly supplying them with the code of the model and the necessary data to run it. We also benefited greatly from several discussions with Dr. V. Krishnamurthy. The authors thank Dr. David Battisti and two other reviewers for some constructive comments and suggestions. Partial support for one of the authors (BNG) comes from the Department of Ocean Development, India through a project. BNG also thanks Dr. D. Sengupta for some suggestions.

REFERENCES

Anderson, D. L. T., and J. P. McCreary, 1985: Slowly propagating disturbances in a coupled ocean–atmosphere model. *J. Atmos. Sci.*, **42,** 615–629.

Barnett, T. P., N. Graham, M. Cane, S. Zebiak, S. Dolan, J. O'Brien, and D. Legler, 1988: On the prediction of the El Niño of 1986–1987. *Science,* **241,** 192–196.

Battisti, D. S., 1988: Dynamics and thermodynamics of a warming event in a coupled tropical atmosphere–ocean model. *J. Atmos. Sci.*, **45,** 2889–2919.

——, and A. C. Hirst, 1989: Interannual variability in the tropical atmosphere/ocean system: Influence of the basic state and ocean geometry. *J. Atmos. Sci.*, **46,** 1687–1712.

Bjerknes, J., 1969: Atmospheric teleconnections from the equatorial Pacific. *Mon. Wea. Rev.*, **97,** 163–172.

Cane, M. A., 1986: El Niño. *Ann. Rev. Earth Planet Sci.*, **14,** 43–70.

——, and S. Zebiak, 1985: A theory for El Nino and Southern Oscillation. *Science,* **228,** 1085–1087.

——, and ——, 1987: Prediction of El Nino events using a coupled model. *Atmospheric and Oceanic Variability.* H. Cattle, Ed., Royal Meteorologic Society, 153–181.

——, ——, and S. C. Dolan, 1986: Experimental forecasts of El Niño. *Nature,* **321,** 827–832.

Gill, A. E., 1980: Some simple solutions for heat induced tropical circulation. *Quart. J. Roy. Meteor. Soc.*, **106,** 447–462.

Goldenberg, S. O., and J. J. O'Brien, 1981: Time and space variability of tropical Pacific wind stress. *Mon. Wea. Rev.*, **109,** 1190–1207.

Goswami, B. N., and S. Selvarajan, 1991: Convergence feedback and unstable low frequency oscillations in a simple coupled ocean–atmosphere model. *Geophys. Res. Lett.* **18,** 991–994.

——, and J. Shukla, 1991: Predictability of a coupled ocean–atmosphere model. *J. Climate,* **4,** 3–22.

Held, I. M., and M. J. Suarez, 1978: A two-level primitive equation atmospheric model designed for climatic sensitivity experiments. *J. Atmos. Sci.*, **35,** 206–229.

Lindzen, R., and S. Nigam, 1987: On the role of sea surface temperature gradients in forcing low level winds and convergence in the tropics. *J. Atmos. Sci.* **44,** 2418–2436.

McCreary, J. P., Jr., 1983: A model for tropical ocean atmosphere interactions. *Mon. Wea. Rev.*, **111,** 370–387.

——, and D. L. T. Anderson, 1984: A simple model of El Niño and Southern Oscillation. *Mon. Wea. Rev.*, **112,** 934–946.

Rasmusson, E. M., and T. H. Carpenter, 1982: Variations in tropical sea surface temperatures and surface wind fields associated with the Southern Oscillation and El Niño. *Mon. Wea. Rev.*, **110,** 354–384.

——, and J. M. Wallace, 1983: Meteorological aspects of the El Niño/Southern Oscillation. *Science,* **222,** 1195–1202.

——, and P. A. Arkin, 1985: Interannual climate variability associated with the El Niño/Southern Oscillation. *Coupled Ocean Atmosphere Models.* J. C. J. Nihoul, Ed., *Elsevier Oceanographic Series,* **40,** Elsevier Publishers, 697–725.

Schopf, P. S., and M. A. Cane, 1983: On equatorial dynamics, mixed layer physics and sea surface temperature. *J. Phys. Oceanogr.*, **13,** 917–935.

——, and M. J. Suarez, 1988: Vacillations in a coupled ocean–atmosphere model. *J. Atmos. Sci.*, **45,** 549–566.

Suarez, M. J., and P. S. Schopf, 1988: A delayed action oscillator for ENSO. *J. Atmos. Sci.*, **45,** 3283–3287.

Wright, P. B., J. M. Wallace, T. P. Mitchell, and C. Deser, 1988: Correlation structure of the El Niño/Southern Oscillation phenomenon. *J. Climate,* **1,** 609–625.

Zebiak, S. E., and M. A. Cane, 1987: A model El Niño/Southern Oscillation. *Mon. Wea. Rev.*, **115,** 2262–2278.

——, and ——, 1988: Diagnostic studies of a coupled model's climate variability. *Proc. 13th Climate Diagnostics Workshop.* Atmospheric and Environmental Research, Inc., Cambridge, Massachusetts, U.S. Dept. of Commerce, 283–288.